

# Thundercloud Electric Fields in the Ionosphere

C. G. Park and M. Dejnakarintra

With 6 figures and 1 table

## Abstract

We consider the problem of electric field mapping around thunderclouds, with particular emphasis upon ionospheric and magnetospheric implications. Calculated electric field strength at large heights depends critically on atmospheric conductivities as well as on cloud parameters. It is extremely important to include the effects of the geomagnetic field above  $\sim 70$  km altitude. At night, horizontal  $dc$  electric field above a bipolar thundercloud may exceed  $10^{-4}$  V/m at 100 km altitude. Time-varying fields due to lightning discharges are also considered. The recovery time following lightning decreases rapidly with increasing altitude until at 100 km the electric field waveform appears as a sharp pulse with  $\sim 0.1$  sec duration. The peak pulse amplitude may easily exceed  $10^{-4}$  V/m. In the daytime, both  $dc$  and  $ac$  fields are weaker by 1 to 2 orders of magnitude as a result of higher conductivities above  $\sim 50$  km. We conclude that thundercloud electric fields are probably too weak to produce significant electrodynamic effects on the daytime ionosphere, but the nighttime values border on being significant.

## Introduction

If we wish to investigate electrical coupling between the troposphere and the ionosphere, we must abandon the classical *Faraday-cage* model of atmospheric electricity, which allows no electric field to exist in the ionosphere. We replace it with a more realistic model illustrated in Fig. 1b. In this new model, electrical conductivity along the geomagnetic field becomes infinite at ionospheric heights, but the transverse conductivities remain finite. Thus equipotential geomagnetic field lines replace the equipotential electrosphere in the classical model as the upper boundary condition. We will see that conductivity anisotropy cannot be ignored above  $\sim 80$  km, because without it electric fields reaching these altitudes from below would be underestimated by several orders of magnitude.

A question of particular interest to us is whether thundercloud electric fields can reach the ionosphere with sufficient strength to cause significant electrodynamic effects such as formation of field-aligned electron density irregularities or excitation of geomagnetic pulsations. We considered this question in two earlier papers (14, 4) and concluded that under favorable conditions thunderclouds could play an important role. Here we will give some further considerations to this problem based on improved calculations.

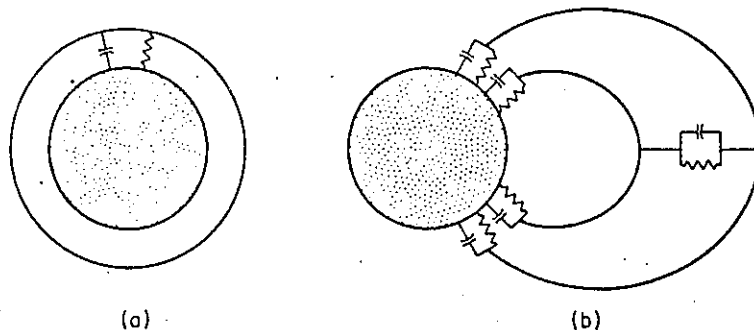


Fig. 1. Sketches illustrating two different conceptual models of geoelectricity. (a) The classical picture in which the earth and the electrosphere, both perfectly conducting, form a leaky spherical capacitor within which atmospheric electricity is confined. (b) A new model in which geomagnetic field lines are assumed to be perfect conductors but the conductivities across field lines remain finite. This model allows electric coupling between the troposphere and the ionosphere/magnetosphere

## Atmospheric Conductivity

Fig. 2 shows mid-latitude conductivity profiles for daytime and nighttime conditions.  $\sigma_{\parallel}$  is the conductivity along the geomagnetic field, and  $\sigma_{\perp}$  is the *Pedersen* conductivity. Above  $\sim 60$  km,  $\sigma_{\parallel}$  and

2026

$\sigma_{\parallel}$  are calculated (16). The nighttime conductivity in the region between the ionosphere and the magnetosphere is assumed to be the same as in the ionosphere.

LOANER - RETURN TO FILES AS SOON AS POSSIBLE!

The basic eq:

and

where  $\Phi$  is the ductivity tensor yield

The  $z$ -axis potential in the isotropic region. We divide the conductivity. For reference altitude.

where

$J_{\parallel}$  is the zero-order constants to be and  $E_z = -\partial\phi/\partial z$

$\sigma_p$  are calculated from recent electron density data (8) together with the U.S. Standard Atmosphere (16). The nighttime model is intended to represent the lowest values to be expected near local midnight. The conductivity profile below 40 km is based on a number of in situ measurements (15, 10, 11, 12, 1). The region between 40 km and 60 km has been filled in to join the upper and the lower curves smoothly.

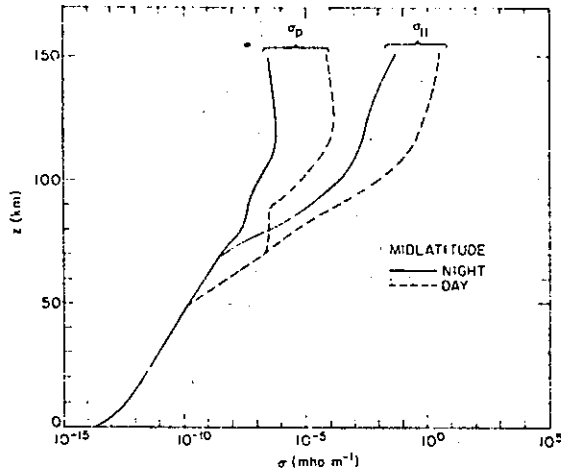


Fig. 2. Midlatitude conductivity profiles for nighttime and daytime conditions.

### DC Electric Fields

The basic equations to be solved are

$$\nabla \cdot \mathbf{j} = 0 \quad [1]$$

$$\mathbf{j} = \sigma \mathbf{E} \quad [2]$$

and

$$\mathbf{E} = -\nabla \phi \quad [3]$$

where  $\phi$  is the electric potential,  $\mathbf{E}$  is the electric field,  $\mathbf{j}$  is electric current density, and  $\sigma$  is the conductivity tensor. If we assume a vertical geomagnetic field, eqs. [1], [2], and [3] can be combined to yield

$$\frac{\partial^2 \phi}{\partial r^2} + \frac{1}{r} \frac{\partial \phi}{\partial r} + \frac{1}{\sigma_p} \frac{\partial}{\partial z} \left( \sigma_p \frac{\partial \phi}{\partial z} \right) = 0. \quad [4]$$

The  $z$ -axis points vertically upward, and an azimuthal symmetry has been assumed.

### Isotropic Region

We divide the isotropic atmosphere below 70 km into several slabs with exponentially varying conductivity. For each such slab, we write  $\sigma = \sigma_p = \sigma_0 e^{(\alpha z - z_0)^2}$ , where the subscript 0 refers to a reference altitude. The solution to eq. [4] for this case can be written as [see (14)]

$$\phi(r, z) = J_0(kr) [A_1 e^{m_1 z} + A_2 e^{m_2 z}] \quad [5]$$

where

$$m_1 = -\frac{1}{2\alpha} - \sqrt{\left(\frac{1}{2\alpha}\right)^2 + k^2}, \quad m_2 = -\frac{1}{2\alpha} + \sqrt{\left(\frac{1}{2\alpha}\right)^2 + k^2}.$$

$J_0$  is the zero-order Bessel function of the first kind,  $k$  is the spatial wave number, and  $A_1$  and  $A_2$  are constants to be evaluated from boundary conditions. Electric fields are obtained from  $E_r = -\partial \phi / \partial r$  and  $E_z = -\partial \phi / \partial z$ .

### Anisotropic Region

If  $\sigma_{\parallel} \neq \sigma_{\perp}$ , but  $\sigma_{\parallel} \propto e^{2\alpha r}$  and  $\sigma_{\perp} \propto e^{2\beta r}$ , it is still possible to find analytical solutions to eq. [4] (14). However, in this case the solutions may involve *Bessel* functions of fractional order, and this method becomes impractical if more than two or three layers are required to adequately represent the conductivity profile. Here we use an alternative approach which allows more accurate calculations with greater economy. We divide the anisotropic regions into a large number of thin (1 km thickness has been found satisfactory) homogeneous layers so that within each layer eq. [4] can be rewritten as

$$\frac{\partial^2 \phi}{\partial r^2} + \frac{1}{r} \frac{\partial \phi}{\partial r} + \frac{\sigma_{\parallel}}{\sigma_{\perp}} \frac{\partial^2 \phi}{\partial z^2} = 0. \quad [6]$$

This equation has the solution

$$\phi(r, z) = J_0(kr) [B_1 e^{i \sigma_{\parallel}^{1/2} z} + B_2 e^{-i \sigma_{\parallel}^{1/2} z}] \quad [7]$$

which involves only simple exponential functions of  $z$ .  $B_1$  and  $B_2$  must be evaluated for each layer from boundary conditions. Although this method requires a large number of layers, numerical calculations are generally easier than in the case of exponential conductivity. Electric fields are again obtained from  $E_r = -\partial\phi/\partial r$  and  $E_z = -\partial\phi/\partial z$ .

### Boundary Conditions

Eqs. [5] and [7] are subject to the following boundary conditions: (i)  $\phi = 0$  at  $z = 0$ , (ii)  $E_z = 0$  at 150 km, (iii)  $E_z$  jumps by an amount  $Q/\epsilon_0$  where the cloud charge  $Q$  is located, (iv)  $E_r$  is continuous across all layer boundaries, and (v)  $J_z$  is continuous across all layer boundaries. Details of mathematical derivation and boundary condition matching can be found elsewhere (3).

### Results

Electric fields are calculated for three different thundercloud models. Model A has +50 coulombs at  $z = 10$  km and -50 C at  $z = 5$  km. In model B, the lower charge at 5 km is increased to -195 C while the upper charge of +50 C remains at 10 km. This is done to make the magnitude of charge proportional to local resistivity so that currents flowing from these charges will be equal (6). Model C, with +50 C at 15 km and -50 C at 5 km, is intended to represent unusually tall clouds that may extend from a few km to 20 or more km [e.g. (17, 18)].

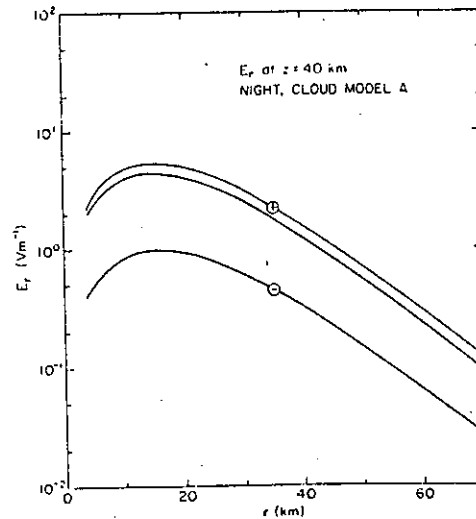


Fig. 3a. Horizontal electric field strength at 40 km altitude plotted as a function of horizontal distance from a model thundercloud. (See text for details)

Fig. 3 shows positive when at 10 km and 5 unmarked curve assumed to be  $-4 \times 10^{-2}$  V/m with Fig. 3b, with from the thund

Fig. 4 shows but its horizon  $E_r$  and  $E_z$  vary above  $\sim 80$  km field. Without a curve parallel

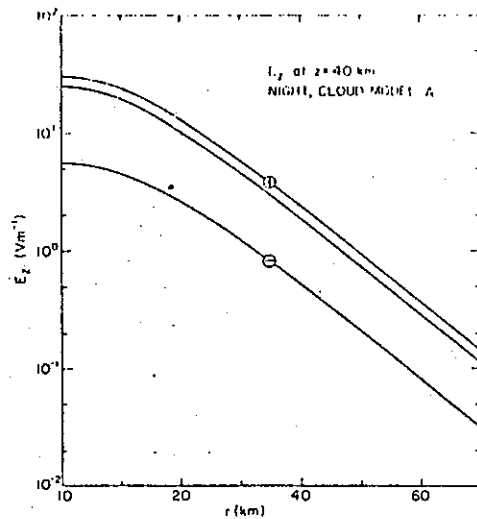


Fig. 3b. Vertical electric field corresponding to Fig. 3a

Fig. 3 shows plots of  $E_r$  and  $E_z$  at  $z = 40$  km.  $E_r$  is positive along the radius vector  $r$ , and  $E_z$  is positive when directed upward. The curves marked (+) and (-) show electric fields due to  $\pm 50$  C at 10 km and 5 km, respectively. When the (-) curves are subtracted from the (+) curves, the resulting unmarked curves represent net electric fields due to cloud model A. If the ionospheric potential is assumed to be 200 kV with respect to the earth, then we predict a downward "fair weather" field of  $4 \times 10^{-2}$  V/m at  $z = 40$  km. (Columnar resistance is  $1.3 \times 10^{17}$  ohms from Fig. 2.) Comparing this with Fig. 3b, we see that "foul weather" should be indicated as far as  $\sim 80$  km horizontal distance from the thundercloud.

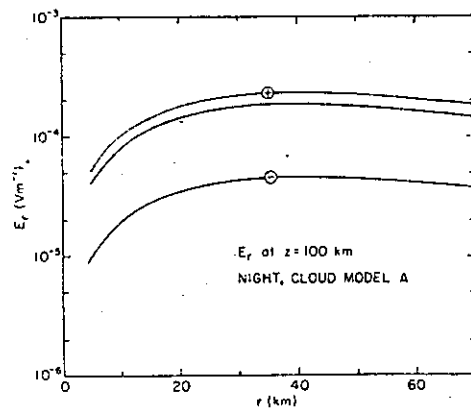


Fig. 4. Horizontal electric field at 100 km altitude corresponding to Fig. 3

Fig. 4 shows  $E_r$  at  $z = 100$  km in the same format as Fig. 3a. The magnitude of  $E_r$  is greatly reduced, but its horizontal distribution is much broader than at  $z = 40$  km. Fig. 5 shows how the maxima of  $E_r$  and  $E_z$  vary with altitude. An important feature to note here is that  $E_{r,max}$  becomes almost constant above  $\sim 80$  km altitude. This is due to the conductivity anisotropy introduced by the geomagnetic field. Without the geomagnetic field,  $E_{r,max}$  would continue to decrease rapidly with altitude following a curve parallel to the  $E_{z,max}$  curve.

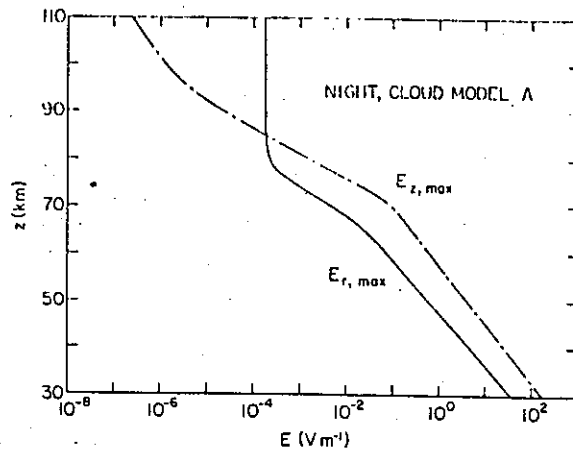


Fig. 5. Plots of maximum horizontal and vertical electric fields as a function of altitude above a model thundercloud. (See text for details)

Table 1 summarizes  $E_{r,max}$  and  $E_{z,max}$  for different cloud and conductivity models. There is very little day-night difference in  $E_{r,max}$  and  $E_{z,max}$  at 40 km altitude, but at 100 km the daytime values are about 2 orders of magnitude less than the corresponding nighttime values. We conclude from these results that in the daytime *de* thundercloud electric fields are too weak to produce significant effects on the ionosphere. The nighttime picture, on the other hand, is quite different. It was shown by Park and Helliwell (13) that electric fields of only  $5 \times 10^{-4}$  V/m in the ionosphere can form ducts for radio waves in  $\sim 1$  hr. Since this level is approached at night by cloud models A and C, thunderclouds cannot be ruled out as a source of localized electric fields in the nighttime ionosphere.

Table 1. Maximum horizontal ( $E_r$ ) and vertical ( $E_z$ ) field strength at various heights for various models of cloud and conductivity

Cloud Model	$E_{r,max}$ at $z = 40$ km		$E_{z,max}$ at $z = 40$ km		$E_{r,max}$ at $z = 100$ km	
	Day	Night	Day	Night	Day	Night
Model A	4.3 V/m	4.4 V/m	24.6 V/m	24.4 V/m	$1.8 \times 10^{-6}$ V/m	$1.9 \times 10^{-4}$ V/m
Model B	1.6	1.6	8.2	8.2	$5.0 \times 10^{-7}$	$6.3 \times 10^{-5}$
Model C	13.6	14.0	74.7	74.3	$4.9 \times 10^{-6}$	$4.9 \times 10^{-4}$

#### Time-Varying Electric Fields

For time-varying fields of the form  $e^{i\omega t}$ , we write the Maxwell's equations as

$$\begin{aligned}\nabla \times \mathbf{E} &= -i\omega\mu_0\mathbf{H} \\ \nabla \times \mathbf{H} &= \sigma\mathbf{E} + i\omega\epsilon_0\mathbf{E}.\end{aligned}$$

From these equations, we obtain an inhomogeneous wave equation

$$\nabla^2 \mathbf{E} + (k^2 - i\omega\mu_0\sigma)\mathbf{E} = \nabla(\nabla \cdot \mathbf{E}). \quad [8]$$

#### Isotropic Region

Below 70 km, we again divide the atmosphere into several layers within which we can write  $\sigma_{\parallel} = \sigma_{\perp} = \sigma_0 e^{(z-z_0)/\lambda}$ . With this approximation, eq. [8] can be solved analytically [see (4) for details of mathematical analysis].

#### Anisotropic Region

In this case, eq. [8] is more difficult to deal with than in the isotropic case, but it turns out that the problem can be greatly simplified if we are interested in frequencies not much greater than 10 Hz. Dejmakarindra (3) used a perturbation method to solve eq. [8] by writing

and

The zero- and radiat exceed  $\sim 6$  involving "tack on" [e.g. (3, 5, 7)]

Boundary c

The bou must be m

Results

It can be increases, J-propagates the recover observed a

Fig. 6. (a) W

Fig. 6 illustrates time variat exponential and  $-20^\circ\text{C}$  the upper c sharp spike are obtaine tude less. T which after nomenon c

It appea significant combined v magnetosp also be ma needed to c

This rese grant GA-28

$$E = E_0 + E_1 + E_2 + \dots$$

and

$$H = H_0 + H_1 + H_2 + \dots$$

The zero-order fields,  $E_0$  and  $H_0$ , are electrostatic fields, while the higher order terms are due to induction and radiation. It was shown that in the altitude and frequency ranges of our interest  $|H_1/E_0|$  does not exceed  $\sim 0.01$ . We can therefore reduce eq. [8] to a set of electrostatic equations by ignoring all terms involving  $\omega$ . After the electric fields have been found by the method of the previous section, we can "tack on" the time variation  $e^{i\omega t}$ . At much higher frequencies, higher-order terms have to be included [e.g. (3, 5, 2)].

#### Boundary Conditions

The boundary conditions are identical to the *dc* case except that in condition (iii)  $E_z(\omega)$  and  $Q(\omega)/\epsilon_0$  must be matched for each *Fourier* component.

#### Results

It can be shown that the atmosphere transmits electric fields upward more efficiently as the frequency increases (4). As a result, high frequency components become more prominent as the disturbance propagates upward. In the time domain, this means that when the electric field waveform is synthesized the recovery time following a lightning discharge decreases with altitude. Such behavior has been observed at balloon altitudes (1, 9).

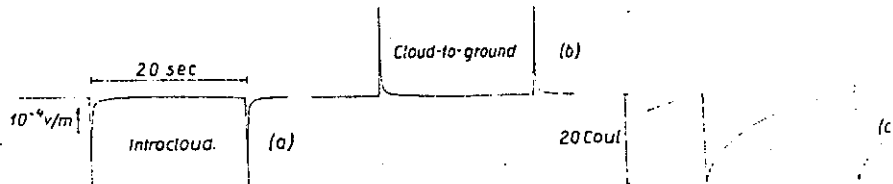


Fig. 6. (a) Waveform of  $E$ , at  $r = 40$  km and  $z = 100$  km due to intracloud discharges. (b) Waveform of  $E$ , due to cloud-to-ground discharges. (c) Assumed time variation of cloud charge

Fig. 6 illustrates the results of sample calculations for nighttime conditions. Fig. 6c shows assumed time variations of cloud charge centers: a lightning discharge occurs in 0.18 second, followed by an exponential recovery with 7-second time constant. Intra-cloud discharges remove  $+20$  C at 10 km and  $-20$  C at 5 km simultaneously, while cloud-to-ground discharges remove  $-20$  C at 5 km, leaving the upper charge undisturbed. In both types of discharges, electric fields at 100 km altitude appear as sharp spikes of  $\sim 100$  msec duration with peak amplitude of  $\sim 3 \times 10^{-4}$  V/m. Similar waveforms are obtained for daytime conductivities, but the corresponding amplitudes are about an order of magnitude less. These fields should be investigated further as a possible source of hydromagnetic waves, which after entering the magnetosphere can be amplified by energetic particles and produce the phenomenon called geomagnetic pulsations [e.g. (7)].

#### Discussion and Concluding Remarks

It appears from the sample calculations that ordinary daytime thunderclouds cannot produce significant electric fields in the ionosphere, but there is a possibility that unusually energetic clouds combined with low nighttime conductivities can cause significant perturbations in the ionosphere and magnetosphere. It would seem worthwhile to look for such effects experimentally. More efforts should also be made to measure electric fields and conductivities above thunderclouds so that the parameters needed to calculate electric fields at higher altitudes can be better defined.

#### Acknowledgments

This research was supported by the National Science Foundation, Atmospheric Sciences Section under grant GA-28042.

## References

1. Benbrook, J. R., J. W. Kern, and W. R. Sheldon, submitted to *J. Geophys. Res.* (1974). — 2. Boström, R., U. Fahlsson, L. Olansson, and G. Hallendal, Tech. Rept. TRITA-EPP-73-02 Royal Institute of Technology (Stockholm, 1973). — 3. Dejnakaritra, M., Ph. D. Thesis, Tech. Rept. No. 3454-3, Radioscience Laboratory, Stanford University (Stanford, 1974). — 4. Dejnakaritra, M. and C. G. Park, *J. Geophys. Res.* **79**, 1903 (1974). — 5. Lamudi, F. and J. R. Wait, *Can. J. Phys.* **49**, 447 (1971). — 6. Holzer, R. E. and D. S. Saxon, *J. Geophys. Res.* **57**, 207 (1952). — 7. Jacobs, J. A., *Geomagnetic Micropulsations* (New York, 1970). — 8. Maeda, K., *J. Geomag. Geoelect.* **23**, 133 (1971). — 9. Manka, R. H. and F. S. Mozer, personal communication. — 10. Morita, Y., H. Ishikawa, and M. Kanada, *J. Geophys. Res.* **76**, 3431 (1971). — 11. Mozer, F. S., *Pure and Appl. Geophys.* **84**, 32 (1971). — 12. Paltridge, G. W., *J. Geophys. Res.* **70**, 2751 (1965). — 13. Park, C. G. and R. A. Helliwell, *Radio Science* **6**, 299 (1971). — 14. Park, C. G. and M. Dejnakaritra, *J. Geophys. Res.* **78**, 6623 (1973). — 15. Saqalyn, R. C. and D. R. Fitzgerald, in *Handbook of Geophysics and Space Environments*, Office of Aerospace Research, U.S. Air Force (1965). — 16. U.S. Standard Atmosphere Supplements, U.S. Government Printing Office (Washington, D.C., 1966). — 17. Vinnipeg, B. and C. B. Moore, *Recent Advances in Atmospheric Electricity*, ed. L. G. Smith, 399 (London, 1958). — 18. Workman, G. J., *Problems of Atmospheric and Space Electricity*, ed. S. C. Coroniti, 296 (New York, 1965).

## Discussion

Ruhnke, Reston, Virginia, USA:

Is your model one- or two-dimensional, and is the magnetic field, as assumed, constant in slope and magnitude?

Park, Stanford, California, USA:

This is a 3-dimensional model, although the conductivity varies only with altitude. Magnetic field lines are assumed to be straight; we do not take their curvature into account. We also assumed constant magnetic dip angle.

Ruhnke:

What latitudes do you assume for these calculations?

Park:

Although we have solutions that apply to any dip angle, we have shown results for vertical field lines only. If one goes to lower latitudes where the dip angle is less than 90°, then one gets slightly different numbers.

Ruhnke:

I hope you realize that in the polar regions there are not many thunderstorms.

Park:

The dip angle is close to 90° even at middle latitudes. For example, in northern U.S. and Canada, where there is considerable thunderstorm activity, the magnetic field lines are close to being vertical. Of course, one will get slightly different numbers if one puts in the tilt angle, but I don't think it is important compared to other variables unless one gets close to the equator.

Mühleisen, Ravensburg, West-Germany:

In your last slide you mentioned penetration of field jumps due to lightning into the ionosphere. In the earlier paper of Boström we could see some damping of waves with different frequencies downwards. If I understood your slide and the calculations of Boström's correctly, then we have a different damping downwards and upwards. Is this correct and what is the explanation?

Park:

That is true. Electric fields are transmitted more efficiently in the direction of decreasing conductivity, so mapping down is much more efficient than mapping up. In the time-varying case, Boström showed that higher-frequency electric fields are damped more severely coming down. When mapping up, one finds the reverse situation: damping decreases with frequency.

Takahashi, Boulder, Colorado, USA:

In your calculation, did you consider the source, that is the thunderstorm, to be a function of time?

Park:

Yes, we did. We assumed a time variation of cloud charges, *Fourier*-analysed it, and then calculated electric fields due to each *Fourier* component. Finally, we summed them all up to reconstruct the wave form.

Authors' address:

C. G. Park and M. Dejnakintra  
Radioscience Laboratory  
Stanford University  
Stanford, California, 94305  
USA